Chapter 3. Stratigraphy and Geochronology

3.1. Materials and methods

Field work was carried out during several field campaigns within the states of Morelos and México (see chapter 1). Lithological units were mapped in the field at a scale of 1:10,000 at five localities, recording approximately 30 % of the 180 km^2 of the Tepoztlán Formation within the study area (Fig. 5). The mapped areas were chosen on account of their good outcrop conditions and are supposed to be representative for the geological conditions of the study area as a whole. The remaining area of the study area was mapped through interpretation of arial photographs and satellite images. All data were integrated into a geographic information system (GIS) environment. Furthermore, eight stratigraphic sections, ranging in thickness from 78 to 378 m, were logged and sampled for petrographical, sedimentological and palaeomagnetic analyses (Fig. 5). The sections provide a large and well-constrained sample suite covering all major depositional units and geological characteristics.

The *Malinalco section* (*MA*) is located southeast of Malinalco (18.93°N, 99.48°W). It attains a thickness of 93 m and is mainly composed of tuffaceous sandstones and tuffs with minor amounts of clay- and siltstones.

The *San Andrés 1 section* (*SA1*) with a thickness of 183 m is located north of the village San Andrés (18.95°N, 99.11°W). The lower part of the section is dominated by tuffaceous sandstones and conglomerates and breccias resulting from fluvial and mass flow processes. With increasing altitude more and more primary tuffs enter the system. The top of the section is dominated by primary tuffs and minor amounts of their reworking products in the form of fluvial and debris flow deposits.

The *San Andrés 2 section* (*SA2*; 18.58°N, 99.06°W), 100 m east of SA1 attains a thickness of 92 m. The lower and the middle part are almost completely composed of tuffs which can be correlated quite well with the corresponding strata in SA1. Again, the top of this section shows an increase in fluvial deposits.

The *Tepozteco section* (*TEP*) is located north of Tepoztlán (18.99°N, 99.10°W). The thickness of this section is 378 m. The lower part is clearly dominated by tuffaceous sandstones and conglomerates resulting from gravel bars and sandy channel fillings. Only minor amounts of primary volcanic material, derived from pumice-and-ash and block-and-ash flows, can be recognized. The upper two thirds of the section are dominated by the deposition of coarse tuffaceous breccias, i.e. debris flow deposits resulting from lahars. Primary tuffs constitute only minor amounts in this part of the section. However, in the upper part a thick lava flow can be found. The top of the section is represented by more debris flow deposits with minor amounts of fluvial tuffaceous sandstones.

The *Sombrerito 1 section* (*SO1*), southwest of Tlayacapan (18.94°N, 98.98°W) reaches a thickness of 78 m. The basis of the section forms a thick lava flow with a thickening- and coarsening-upward sequence of tuffaceous sandstones and conglomerates and minor primary tuffs on top.

The *Sombrerito 2 section* (*SO2*; 18.56°N, 98.59°W), is a continuation of SO1 but with a horizontal shift of 100 m towards northwest and attains a thickness of 110 m. In the lower part it is mostly composed of primary volcanic products resulting from pumice-and-ash and block-and-ash flows. With increasing altitude fluvial deposits become more and more dominant with increasing amounts of mass flow deposits to the top.

The *Tonantzin section* (*TO*), in the north of Tlayacapan (18.97°N, 98.98°W) has a thickness of 79 m. Tuffaceous sandstones resulting from sheet-floods and sandy channel-fills dominate the lower part of the section. In the upper part, deposits from pumice-and-ash flows and debris flows are increasingly abundant.

The *San Agustín section* (*TL*) is located northeast of Tlayacapan and just north of San Agustín village (18.99°N, 98.96°W). It attains a thickness of 133 m and is characterised by a steady increase in pyroclastic flow deposits. Deposits from debris flows are abundant whereas fluvial tuffaceous sandstones and conglomerates decrease with increasing altitude within the section. The top of the section is characterised by a thick, blocky lava flow.

Sampling and analytical procedure for K/Ar dating

Here, new $^{40}K/^{40}Ar$ and $^{40}Ar/^{39}Ar$ age data are presented for different dacitic to andesitic lava samples collected within the sections TEP, SO1 and TL. Two more samples were taken close to MA and SA1 and were interpolated into the stratigraphic sections. The mineral content of the samples is listed in Table 1. Furthermore, one lava sample was taken near Ahuatenco (Zemp12) and four samples of pyroclastic rocks were taken in the sections SA1, TEP, SO1 and TL (Tab. 2). However, the results received from the pyroclastic rocks were excluded because of too high alterations of glassy material to clay minerals.

The samples were carefully cleaned and selected in order to avoid alterated parts or veins. The selected pieces were broken and gently milled in a ball mill to reach an appropriate grain size of approx. 100µm to prevent the loss of Ar caused by preparation. The samples investigated suffer from a trapped, atmospheric contamination (up to 90% of the ^{40}Ar) which can not be avoided in most modern volcanic rocks (s. discussion in McDougall and Harrison, 1999). Therefore, errors amount to 15% (2σ). Earlier Ar-Ar ages, taken from Lenhardt (2004) were obtained from bulk rock analysis in a commercial laboratory.

The argon isotopic composition was measured in a pyrex glass extraction and purification line coupled to a VG 1200 C noble gas mass spectrometer operating in static mode. The amount of

radiogenic ^{40}Ar was determined by isotope dilution method using a highly enriched ^{38}Ar spike from Schumacher, Bern (Schumacher, 1975). The spike is calibrated against the biotite standard HD-B1 (Fuhrmann et al., 1987). The age calculations are based on the constants recommended by the IUGS quoted in Steiger and Jäger (1977). Potassium was determined in duplicate by flame photometry using an Eppendorf Elex 63/61. The samples were dissolved in a mixture of HF and HNO_3 according to the technique of Heinrichs and Herrmann (1990). CsCl and LiCl were added as an ionisation buffer and internal standard respectively. The analytical error for the K/Ar age calculations is given on a 95% confidence level (2σ). Details of argon and potassium analyses of the laboratory at the University of Göttingen are given in Wemmer (1991).

Sampling and analytical procedure for palaeomagnetic measurements

From the stratigraphic sections a total of 1087 cores were sampled in 153 horizons for this study, 174 in the MA section (16 horizons), 236 in the two SA sections (40 horizons), 171 in the TEP section (28 horizons), 289 in the two SO sections (37 horizons), 64 in the TO section (11 horizons) and 152 in the TL section (21 horizons; Appendix 2). Between 3 and 12 cores per horizon were collected in average intervals of 10 meters. The samples were collected from tuffs, tuffaceous sandstones, the matrix of tuffaceous breccias and lava. While sampling sediments, it was aimed to drill into zones with fine matrix to eliminate problems due to coarse grain sizes (e.g. Barberà et al., 2001). The most common way to extract drill cores is with the help of a gasoline-driven drilling machine with diamond-studded drill heads. The diameter of the drill cores usually is 2.5 cm but drill cores of 1.2 cm in diameter were also taken. After drilling up to a depth of 6 – 12 cm, an orientation platform is slipped onto the sample while the latter is still attached to the surrounding rock. The orientation platform contains an inclinometer for the determination of the inclination of the solid axle and a magnetic as well as a sun compass for the determination of the azimuths of the solid axle. The error of the directional reference is about ± 2°. After orientation, the drill core is taken from the outcrop, labelled and taken to the laboratory for further treatment.

The natural remanent magnetization (NRM) of all samples was analysed with the help of an AGICO JR5 induction magnetometer at the Centro de Geociencias, UNAM, Querétaro, Mexico. The samples were demagnetised using stepwise alternating field (AF) treatment in field amplitudes up to 100 mT using an AGICO LDA instrument. Remanence components were identified from orthogonal demagnetization plots (Zijderveld, 1967) and best fits determined using principle component analysis. Site mean directions were calculated using Fisher (1953) statistics (Appendix 3).

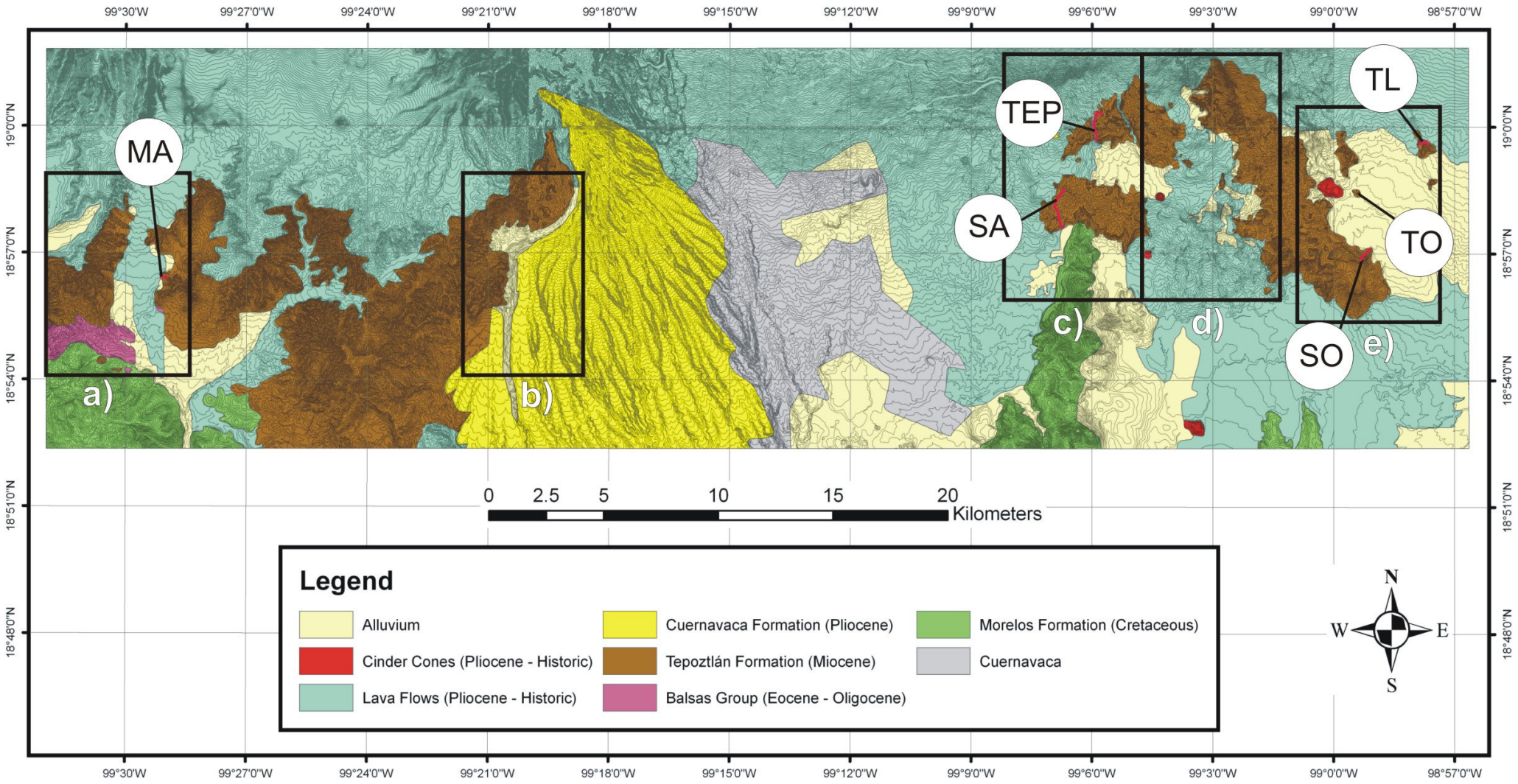

Figure 5. Geological map with locations of the sampled sections (red lines), based on the maps (black frames) of a) Michelson and Tunon-Vettermann (2004), b) Cizmezcia (in prep.), Faridfar (2009), Lehmann (2009), c) Lenhardt (2002), d) Hechler (2002), e) Bär and Schwab, (2005).

3.2. Results

Geochronology

The radiometric ages obtained (Tab. 2 and 3) for the Tepoztlán Formation range between 21.8 ± 0.2 Ma and 19.8 ± 0.8 Ma. This corresponds to the initial phase of the TMVB as stated by Gómez-Tuena et al. (2007). Because of the described errors, single data have only a minor significance. This deficiency however, can be counterbalanced by palaeomagnetic and lithologic correlation.

Table 2: Data base of K–Ar age determinations

Sample	Spike [No.]	K_2O [Wt. %]	40 Ar * [nl/g] STP	40 Ar * [%]	Age [Ma]	2δ-Error [Ma]	2 δ -Error [%]
M 210	3763	0.66	0.447	10.03	**20.9**	3.1	14.8
TL 250-5p	3759	1.16	0.752	20.91	**20.0**	1.0	5.0
TE 5	3747	1.31	0.822	16.76	**19.4**	1.2	6.2
TL 233-12p	3743	1.33	0.853	28.48	**19.8**	0.1	0.4
Zemp 12	3898	1.32	0.9362	46.55	**21.9**	0.5	2.3
SA 18	3745	1.54	0.611	13.26	**12.3**	0.9	7.3
TE 4	3742	0.75	0.388	27.83	**15.9**	0.6	3.8
TE 5	3741	1.31	0.806	16.55	**19.0**	1.2	6.3
SO 14	3756	0.71	0.613	7.27	**26.6**	3.7	13.9
TL 6	3762	0.24	0.115	11.64	**14.8**	1.5	10.1

Table 3: Data base of Ar-Ar age determinations

Sample	J	Weight (mg)	MSWD	$^{40}Ar/^{36}Ar$	% ^{39}Ar used	Age (Ma)
SAC	0.001020 ± 0.000008	124.0	0.18/ 2.63	449.84 ±12.89	61.7	**21.86 ± 0.20 Ma**
DI1	0.001014 ± 0.000010	88.0	0.41/ 3.83	319.32 ± 16.3	8.5	**15.83 ± 1.31 Ma**

J is the irradiation parameter; MSWD is the mean square weighted deviation (Wendt and Carl, 1991), which expresses the goodness-of-fit of the isochron. (Roddick, 1978).

Palaeomagnetic analysis

NRM intensities range between low 0.00059 and 81.16 A/m (average 1.47 A/m). The ferromagnetic minerals within the samples are predominantly titanomagnetites with a relatively low content in titanium as was observed during palaeomagnetic measurements and SEM studies (Lenhardt, 2004).

Typical examples of AF demagnetization diagrams are shown in Fig. 6 as orthogonal projections of magnetization vectors. The NRM of the samples mainly consists of one dominating magnetization component, with a small unstable contribution which is removed

during the first AF demagnetization steps (0-20 mT). In occasions more than two magnetization components were observed, and the characteristic direction was then assigned taking into account the overall behaviour of samples from the entire outcrop. All characteristic directions were defined using principal component analysis (Kirschvink, 1983). The examples shown in Fig. 6 are from the main depositional environments, and the quality of the demagnetization data is clearly related to the temperature during deposition. The lava sample SO67-76 exhibits a strong univectorial thermoremanent magnetization component. All other samples in comparison are demagnetised faster at low AF steps, and their directional behaviour along the demagnetization process is also more dispersed. Nevertheless, in most cases a characteristic remanence direction may be determined with sufficient precision for assigning a magnetic polarity.

These characteristic remanent magnetization directions were used to calculate site-mean directions and virtual geomagnetic poles (VGP). Geomagnetic polarity was determined by the VGP latitude, being normal (reverse) for positive (negative) latitude.

Often, within-site dispersion of directions was large, with confidence limits α_{95} between 2.3° and almost 90°. At many sites this was related to the coarse grain size of the included particles, and it also occurred that part of the samples showed well grouped magnetic directions and several other samples a clearly divergent direction. This is interpreted to reflect the variability of grain sizes and depositional processes involved, mainly in the fluvial sediments. Here, the inclusion of up to granule sized particles, which are not oriented by the geomagnetic field, may produce a remanence direction deviating from the ambient field direction. Samples with confidence limits α_{95} higher than 45° were thus considered as unconfined and were not taken for further analysis. Dispersion is lowest in lavas (mean α_{95} 13.2°) and highest in fluvial deposits (mean α_{95} 29.5°). Tuffs are characterised by a mean α_{95} 26.3°. Surprisingly, deposits interpreted as mass flow deposits have a relatively low mean α_{95} with 23.8° which is lower than the calculated mean value for the tuffs which had been deposited under higher temperature conditions. However, the relatively low values might be due to smaller grain sizes which make up the matrix of the mass flow deposits in contrast to pumice-bearing tuffs.

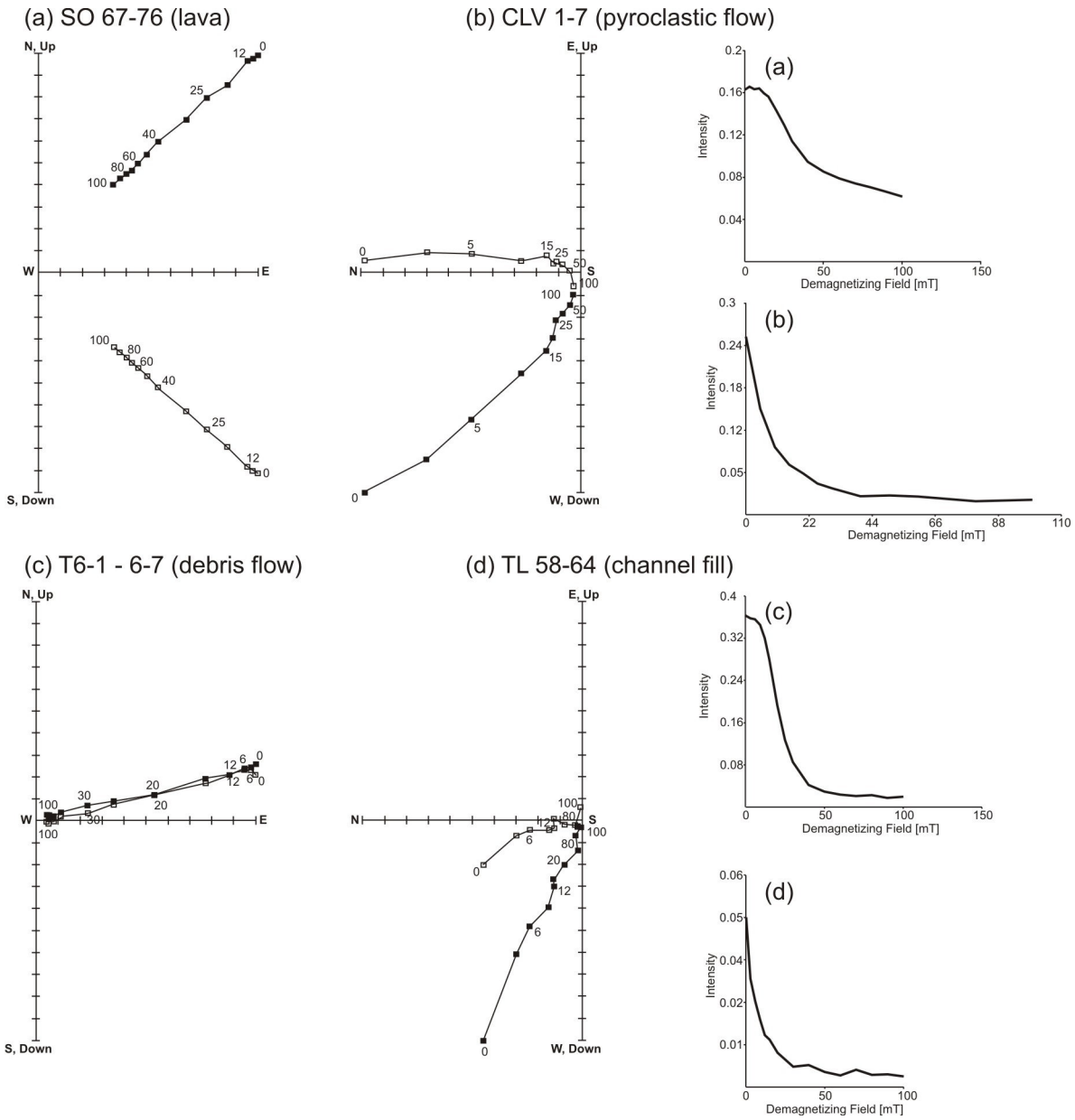

Figure 6. Examples of orthogonal vector (Zijderfeld) plots of four samples undergoing alternating-field demagnetization. Each plot shows the projection of the magnetization vector endpoint on two perpendicular planes, one in the horizontal plane (solid symbols) and one vertical (open symbols). Numbers give strength of the demagnetizing field in milliTeslas (mT). To the right, intensity plots of the samples are shown.

Remanence acquisition for lava (depositional temperature above 600°C) and tuff (depositional temperature between 200 and 400°C) was through thermoremanent magnetization (TRM), and is acquired by a rock during cooling from a temperature above Curie temperature in an external magnetic field (Merrill et al., 1998). Fluvial and mass flow deposits (deposition at ambient air temperature) are characterised by detrital or depositional remanent magnetization (DRM), acquired by sediments when grains settle in water in the presence of an external magnetic field (Merrill et al., 1998).

Comparison of the data before and after demagnetization showed that the chosen polarity of NRM did not change after demagnetization. Therefore, it is assumed that the undemagnetised samples indeed contain a NRM direction which may be used for magnetostratigraphy purposes.

Local magnetic polarity stratigraphies (LMPS) were constructed for the individual sections and compiled into a single composite section covering a net of ~577 m of strata. Correlation between the combined sections MA, SA1, SA2, TEP, SO1, SO2, TO and TL yields a composite LMPS containing 14 reversals. These reversals are correlated to the age models of Cande and Kent (CK95; 1995). Considering the age constraints given by K-Ar and Ar-Ar geochronology (including their errors), this allows a correlation to (sub)chrons 6Bn.1n - 5Er, covering a time span of ~3.97 Ma for the entire deposition of the Tepoztlán Formation (Fig. 7).

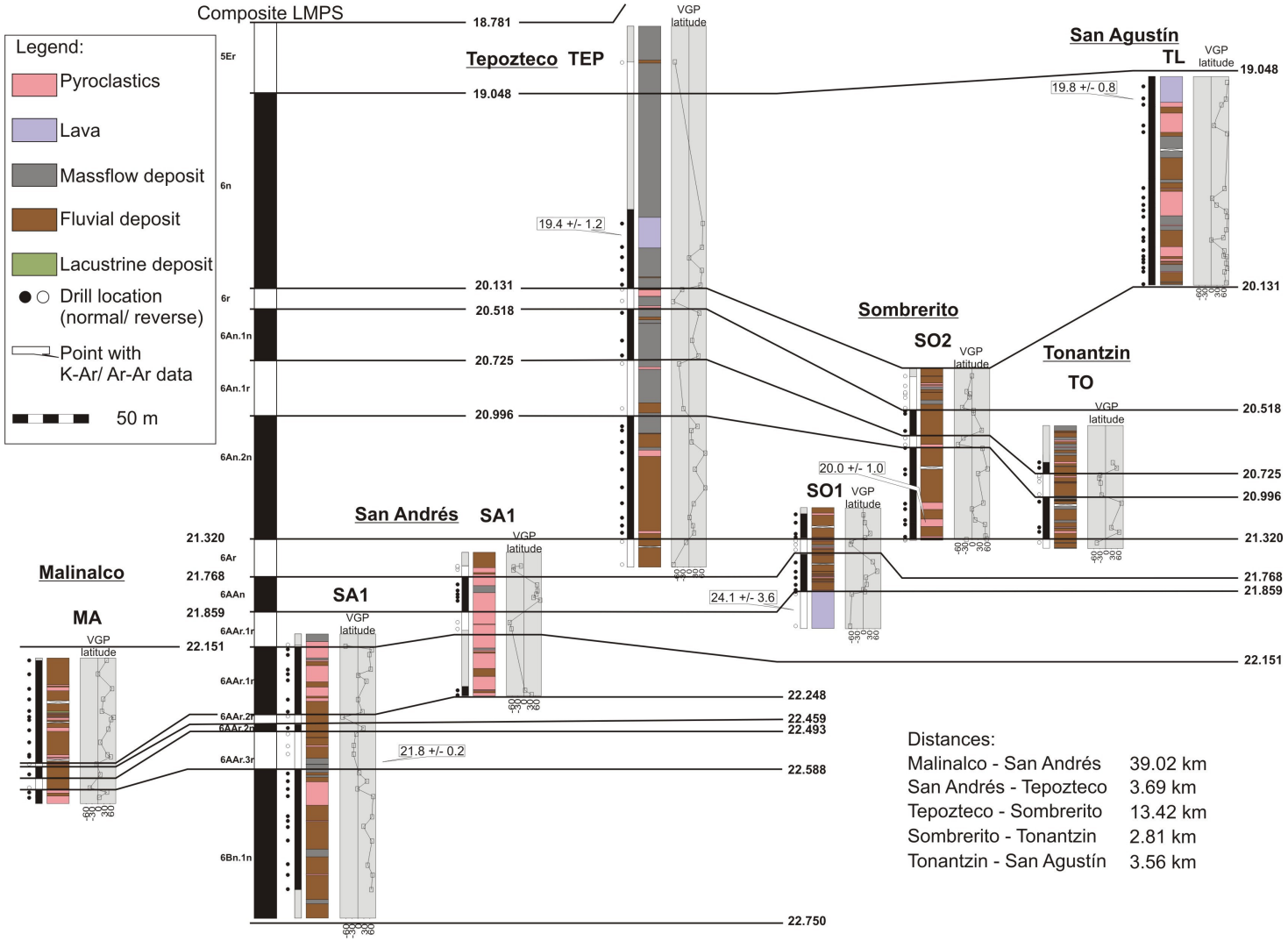

Figure 7. Lithostratigraphic sections of the Tepoztlán Formation with palaeomagnetic and radio-isotopic analysis results and magnetostratigraphic correlation to the geomagnetic polarity time scale of Cande and Kent (CK95; 1995).

3.3. Discussion

Radiometric dating of dacitic lavas within the Tepoztlán Formation yields ages between 21.8 ± 0.2 Ma and 19.8 ± 0.8 Ma. Given the low potassium content of these rocks, it is difficult to tell which age, given by K-Ar and Ar-Ar geochronology is more precise and reliable. However, combined with palaeomagnetic data, the chronostratigraphic study of the Tepoztlán Formation gives much better age constraints for its time of deposition. Considering the radiometric ages together with their errors, the author provides the best possible correlation of the composite LMPS fitting to the CK95 GPTS. This correlates the sections to chrons 6Bn.1n - 5Er in the early Miocene and encompasses a time of deposition between 22.8 and 18.8 Ma (22.8 – 22.2 Ma for MA section, 22.8 – 21.3 Ma for SA1 and SA2 sections, 21.8 – 18.8.0 Ma for TEP section, 22.2 – 20.1 Ma for SO1 and SO2 sections, 21.8 – 20.5 Ma for TO section and 20.1 – 18.8 Ma for TL section; see Fig. 7). Where individual sections overlap via lithostratigraphic correlation the polarity zones are coincident (e.g. SA1 and SA2, SO1 and SO2). This agreement of reversals in nearby lithostratigraphically correlated sections reinforces the robustness of the local (< 500 m) correlations and of the LMPS itself.

The resulting ages coincide with the time of the initial activity of the Transmexican Volcanic Belt as proposed by Gómez-Tuena et al. (2007), compiling the results of several other authors (Pasquaré et al., 1991; Capra et al., 1997; García-Palomo et al., 2000; Ferrari et al., 2003). Pasquaré et al. (1991) and Capra et al. (1997) describe Early Miocene basaltic-andesite lavas from the Sierra de Mil Cumbres and Sierra de Angangueo volcanic complexes in the State of Michoacán, while García-Palomo et al. (2000) and Ferrari et al. (2003) dated volcanic rocks in the Tenancingo and Malinalco areas in the State of México, and in the deepest part of the Mexico City basin. Here, ages ranging between 21.6 and 16 Ma were obtained from basaltic and andesitic lavas. The study shows that the time of deposition of the Tepoztlán Formation fits very well into the time-frame provided by these authors, however, the time of deposition of the Tepoztlán Formation can now be defined more precisely. The formation of the San Nicolás Basaltic Andesite at 21.6 ± 1.0 Ma (García-Palomo, 1998), underlying the Tepoztlán Formation in the Malinalco area, suggests a contemporaneous deposition of both formations within the study area. However, closer field relationships between both formations have not been studied yet. The post-depositional history of the Tepoztlán Formation is characterised by the emplacement of various dykes, yielding ages as young as 15.83 ± 1.31 Ma. This time coincides with a period of plutonic to subvolcanic body emplacement of gabbroic to dioritic composition and ages varying between ca. 15 and 11 Ma (Gómez-Tuena et al., 2003; Ferrari et al., 2005), leading to an episode of fissure eruptions with widespread lava plateaus between the states of Nayarit and Veracruz (Ferrari and Rosas-Elguera, 2000; Ferrari, 2004; Ferrari et al., 2005).

The stratigraphy of the Tepoztlán Formation obtained in the course of this study shows that, due to a misinterpretation of certain deposits and a lack of time markers to correlate the

stratigraphic sections, Haro-Estrop's (1985) subdivision of the formation has to be revised. With the new age constraints and according to the dominant mode of deposition a new subdivision of the Tepoztlán Formation can be proposed. The following lithostratigraphic names are suggested according to the type localities (Fig. 8): (1) a fluvial dominated lower unit (Malinalco Member; 22.8 – 22.2 Ma), (2) a volcanic dominated middle unit (San Andrés Member; 22.2 – 21.3 Ma) and (3) a mass flow dominated upper unit (Tepozteco Member; 21.3 – 18.8 Ma). Sediments near the TL section that were formerly described by Haro-Estrop (1985) as part of the fluvial-laharic unit belonging to the middle part of the sedimentary sequence are now assigned to the youngest sediments within the succession.

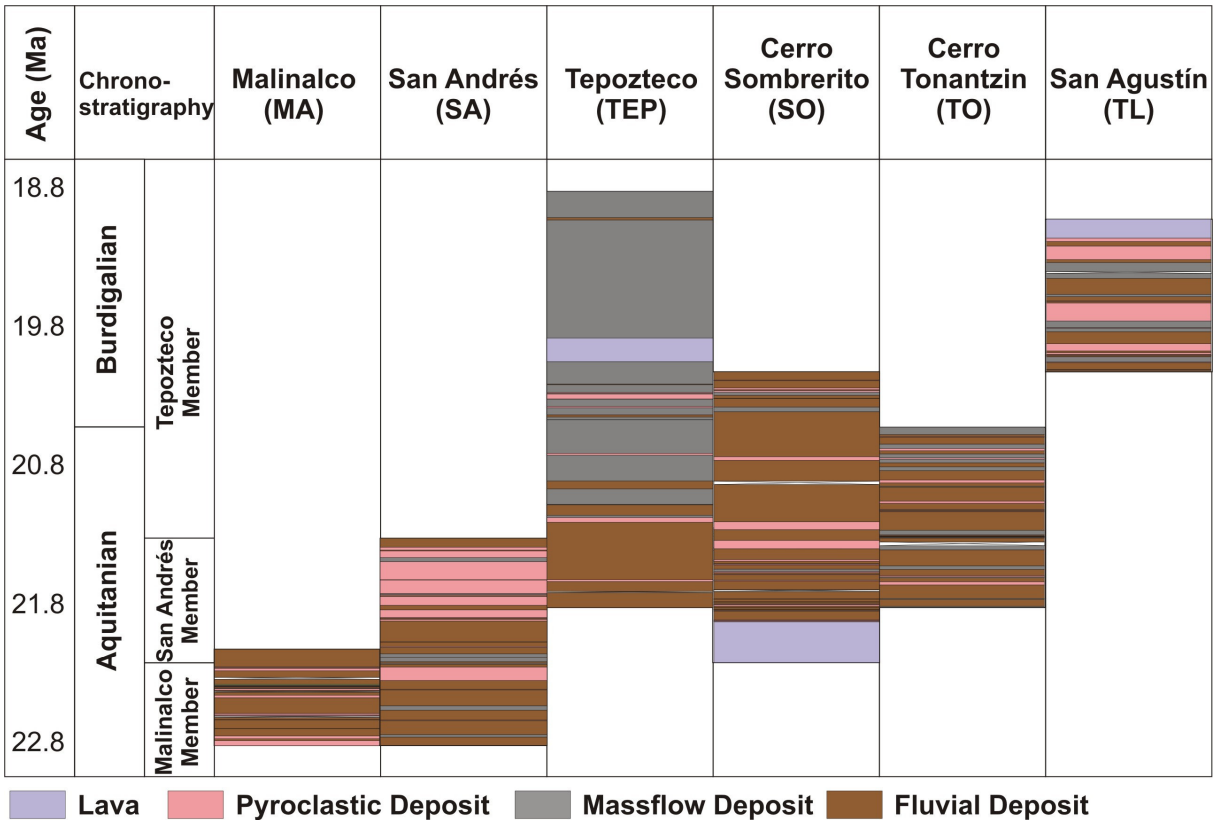

Figure 8. Chronostratigraphical correlation of the stratigraphic sections together with their predominant lithologies.